# POROUS STAINLESS STEEL PARTS USING SELECTIVE LASER SINTERING

Donald F. Heaney and Randall M. German
The Center for Innovative Sintered Products
The Pennsylvania State University
118 Research Building West
University Park, PA 16802
dfh100@psu.edu

## ABSTRACT

Porous stainless steel bodies were fabricated by use of selective laser sintering (SLS). The permeability was varied by modification to the processing parameters. Experiments were performed to determine the effect of powder size and sintering temperature on the final porosity, permeability, and maximum pore size of the stainless steel structures. Large changes in pore structure were obtained by modification to the initial powder size. The permeability was more closely controlled by modification to the sintering temperature. Selective laser sintered parts have a density that is equivalent to slightly less than the apparent density of the metal powder; thus, the permeability is equivalent to the permeability of the unpacked loose powder. This permeability and other porous material characteristics are only modified by densification during high temperature sintering.

## INTRODUCTION

Porous stainless steel finds use in filters, spargers, electrodes, and fluid flow control applications where demanding materials characteristics are required.[1] These are applications that require high strength, rigidity, and corrosion resistance.

Typically, the geometries are limited to simple shapes such as discs, cylinders and cones, unless an expensive and environmentally hazardous process is employed. In this process, the complex porous stainless steel parts are fabricated by machining a block of porous stainless steel to the desired shape. This process closes the surface porosity of the steel because of metal smearing. The pores are then reopened by the use of acid. Significant material and chemical waste is produced by this method. Also, non-uniform surface porosity and undesirably smooth surface are often present.

A net-shape method for the fabrication of these porous materials is presented here. In this method, the shapes are fabricated directly from a computer file by use of selective laser sintering (SLS). A feasibility and process optimization study was conducted to evaluate this process for

(SLS). A feasibility and process optimization study was conducted to evaluate this process for porous stainless steel applications. Two methods, the selection of the initial particle size and the high temperature sintering temperature, were used to modify the porous metal's porosity, permeability, and maximum pore size.

## BACKGROUND

A new rapid prototyping method, selective laser sintering (SLS), is becoming an acceptable method for the production of prototype parts.[2] In a typical application, the part is made from a CAD file. The part is built layer-by-layer using a laser to bond one layer of loose polymer coated powder to the previous laser bonded layer. The completed part is fragile; however, it has enough handling strength for transport to the furnace for debinding and sintering. One method is to pack the part in a course alumina powder to enhance wicking of the polymer from the part and to give the part structural support during sintering. The final step in the "classical SLS process" is to obtain high density by infiltrating the porous materials with a low melting point metal such as copper. This step is required because the coarse powder used to make the parts has limited sinterability and also because densification causes geometric distortion. A new variant of this technology is to eliminate the infiltration step and directly manufacture porous parts. This is a new application for selective laser sintering and shows much promise for the future of net-shape porous part production.

Typically, porous stainless steel bodies are manufactured by machining a block of 50 to 75 % dense sintered powders and by chemical etching the final geometry to open the pores that were closed during machining. The porous structure of the product can be quite variable because of the aggressive nature of the process. The machining may significantly reduce the opened porosity on the surface and the acid may significantly increase the porosity in other regions. Using this new method, porous stainless steel parts can be manufactured to closer tolerances with less waste and shorter lead times.

## EXPERIMENTAL PROCEDURE

Porous stainless steel bodies were fabricated using selective laser sintering (SLS). In this study, the variables were particle size and sintering temperature. The responses were porosity, permeability, and maximum pore size.

UltraFine Powder Technology Inc. gas atomized 316L stainless steel powder was sieved to three different sieve size fractions -- -60/+100, -100/+140, and -200/+270. These sizes were selected because they all flow well and they offer a size range that could produce a meaningful range for the responses. The primary powder characteristic that is required for SLS is flowability. These powders were mixed with an organic binder that is capable of being laser sintered together at a relatively low temperature (<300°C). The organic binder acts as a glue to hold the powders together during the building stage. These prepared powders were then ready for selective laser sintering.

Selective laser sintering was performed using a DTM Corporation Laser Sinterstation 2000. Figure 1 is a schematic diagram of the selective laser sintering process. The coated powder is moved with the roller from the powder storage bin to the build platform at a time interval between each laser treatment. The build platform is directly below the laser where the part is made. Cylinders that were 1.27 cm in diameter and 1.27 cm in height were fabricated for testing and then prototype parts of 7.5 cm diameter and 10 cm in height were fabricated for a fluid flow application. The SLS machine was set up differently for each powder. In this study, the three most significant parameters for the production of quality parts were binder content, laser intensity, and build height. The build height is the distance that the build platform moves down between each laser treatment and powder replenishment step.

The binder content effect is as follows. Too little binder does not permit significant bonding between powder particles; too much binder causes the rollers on the machine to "gum-up" and segregation of the binder from the powder also occurs. When the laser intensity is too high, the polymer burns and the part has cracks in both the vertical and horizontal direction. At low laser intensities, the part does not have a significant amount of handling strength and cracking may appear in the horizontal direction. The build height has the following effects on part quality. If it is too high, the layers do not bond together, if it is too small, a layer of powder does not get left behind for laser treatment and a part of poor integrity is built. The build height was adjusted to approximately twice the size of the D90 particle size. The build height adjustment had the most significant effect on the part quality when moving from one powder size to the next powder size.

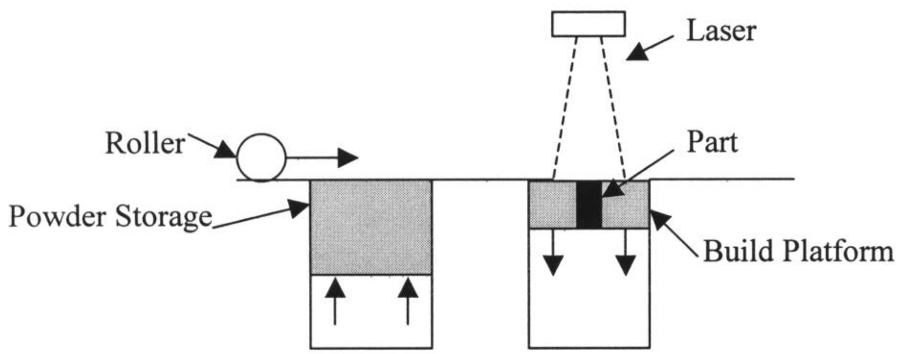


Figure 1. Selective laser sintering schematic diagram.

After SLS, the samples were packed in coarse alumina and then put in an Inconel batch furnace to burn out the binder. The thermal cycle was 5°C/min to 450°C with a hold for 1 hour followed by 5°C/min to 1000°C for presintering with a cover gas of hydrogen. These samples were then sintered in a CM tube furnace for two hours in the temperature range between 1000°C and 1350°C in hydrogen gas.

The resulting samples were then measured for porosity, permeability, and maximum pore size. These tests were chosen since they represent a battery of tests that can be useful for a design engineer to make porous material selection decisions.

The porosity ($\epsilon$) of the samples were calculated as follows:

$$\varepsilon = 1 - \frac{\rho_{geometric}}{\rho_{pycnometry}} \tag{1}$$

The $\rho_{geometric}$ is simply the mass divided by volume for the processed parts. The pycnometry density was measured for each powder size to account for atomization produced entrapped voids as the powder size increased.

The permeability was measured using Darcy's Law. Cylindrical samples were placed in the flow path of air. The pressure drop across the sample was measured and used to calculate permeability as follows[3]:

$$\alpha = \frac{QL\eta}{\Delta PA} \tag{2}$$

where $\alpha$ is the permeability ($m^2$), Q is the gas flow rate ($m^3$/sec), L is the sample length (m), $\eta$ is the gas viscosity ($1.84 \times 10^{-5}$ Nsec/$m^2$), $\Delta P$ is the pressure drop across the sample (Pa), and A is the cross-sectional area of the sample ($m^2$). This equation is valid for air, even though air is compressible. Our test was performed at very low velocity and corresponding to Reynolds numbers near unity or less; therefore, inertial effects are minimal and a second term for nonlinear energy loss is not required.

The maximum pore diameter was calculated using ASTM standard E128. In this method, the maximum pore diameter is calculated by immersing the porous material in alcohol and by applying air pressure until the first bubbles of air appear on the top of the porous material. The maximum pore diameter ($D$) is calculated from the surface tension of the alcohol on the stainless steel ($\gamma$ = 22 dynes/cm) and the applied pressure ($p$) as follows:

$$D = \frac{(30\gamma \times 13.53)}{p} \tag{3}$$

The pressure ($p$) is measured in mm of water on a manometer.

## RESULTS

The powders were characterized for particle size distribution, apparent density and tap density. The results are shown in Table 1. The SLS samples have a density that is less than the apparent density of the virgin powder because if the binder. Therefore, higher density parts can only be fabricated by either high temperature sintering or by modification to the particle packing characteristics.

Table I. Powder Characteristics

| Sieve Mesh Size | D10 (μm) | D50 (μm) | D90 (μm) | Apparent Density ($g/cm^3$) | Tap Density ($g/cm^3$) |
|---|---|---|---|---|---|
| -200/+270 | 38.2 | 49.8 | 67.5 | 4.23 | 4.77 |
| -100/+140 | 41.1 | 64.4 | 106.1 | 4.15 | 4.55 |
| -60/+100 | 125.8 | 173.3 | 233.7 | 4.18 | 4.50 |

The effect of sintering temperature on the permeability of selective laser sintered powders is shown in Figures 2 through 4. The permeability ranged from $3x10^{-12}$ to $6x10^{-12}$ $m^2$ for the powder that had a D50 of 49.8 μm. The permeability ranged from $4x10^{-12}$ to $14x10^{-12}$ $m^2$ for the powder that had a D50 of 64.4 μm. The permeability ranged from $20x10^{-12}$ to $50x10^{-12}$ $m^2$ for the powder that had a D50 of 173.3 μm. As the sintering temperature was increased, the permeability decreased because of sintering densification.

Figures 5 and 6 show the effects of initial powder size on permeability for two different sintering temperatures (1100°C and 1300°C). Modifications to the powder size have the greatest influence on the permeability of a part.

The effect of sintering temperature on the porosity of the three different powder size distributions is presented in Figure 7. The porosity for all three powder size distributions was about 50% after sintering at 1100°C. The coarser powder has a greater initial porosity than does the finer powder. These porosities are greater than the porosity predicted by the apparent density of the powder. This seems to not be logical; however, a decreased density can be explained by the presence of the binder in the SLS process. The porosity of the samples does not change until above 1200°C for all the samples.

The effect of sintering temperature on the maximum pore size of the three different powder size distributions is presented in Figure 8. The maximum pore size remains relatively constant until 1300-1350°C for all three powder size distributions.

## DISCUSSION

The SLS process produces uniform particle packing characteristics. The particles pack to slightly less than the apparent density of the powder. This can be explained by the presence of binder on the powder prior to the process. Since the pore structure of a sample is very sensitive to the packing density of a powder compact, the uniform packing of particles that is inherent to this process is ideal for the production of well-controlled and uniform porosity, permeability, and maximum pore size.

Increasing the sintering temperature can modify the strength of the compact. However, as the sintering temperature is increased, the porosity and permeability are decreased. The permeability of the sample begins to decrease at temperatures above 1100°C. However, the porosity does not decrease until above 1200-1250°C. The smaller powder is more sensitive to the effect on porosity, as should be expected. Interestingly, the maximum pore size remains relatively constant up to a temperature of about 1300°C.

The particle size was shown to have a greater influence than the sintering temperature on the permeability and maximum pore size. Adjustment of sintering temperature more closely controls the porosity. As the sintering temperature increased above 1350°C, the temperature is more dominate as compared to particle size on the permeability and maximum pore size. This is a result of liquid phase sintering at these temperatures.

## CONCLUSIONS

Porous stainless steel samples have been fabricated using SLS. An engineering tool for the production of net shape porous materials is defined in this paper. The SLS method has proven to be effective for the production of well-controlled porous structures. Expensive machining and chemical pore opening procedures are avoided. The pore structure is effectively controlled by the use of initial particle size and sintering temperature. Temperatures above 1350°C should be avoided since liquid phase sintering dominates and causes rapid densification and poor control of permeability. A temperature of 1250-1300°C is recommended to obtain sufficient strength for porous SLS parts. The pore structure is then modified by the use of different sized powders. Also, by using the SLS process, the surface roughness is better suited for fluid flow boundary layer applications (as shown in Figure 9).

Table II: Approximate properties at a sintering temperature of 1250°C and a sintering time of 2 h for all three powder distributions.

| **Powder D50 (μm)** | **Porosity (%)** | **Permeability ($m^2$)** | **Max Pore Size (μm)** |
|---|---|---|---|
| 49.8 | 43 | $3.9 \times 10^{-12}$ | 50 |
| 64.4 | 46 | $12 \times 10^{-12}$ | 80 |
| 173.3 | 48 | $27 \times 10^{-12}$ | 140 |

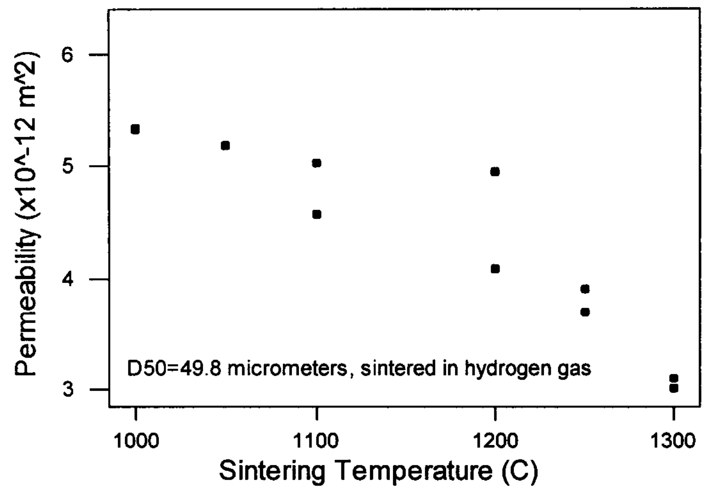


Figure 2. The effect of sintering temperature on the permeability of selective laser sintered D50=49.8 μm 316 stainless steel powder.

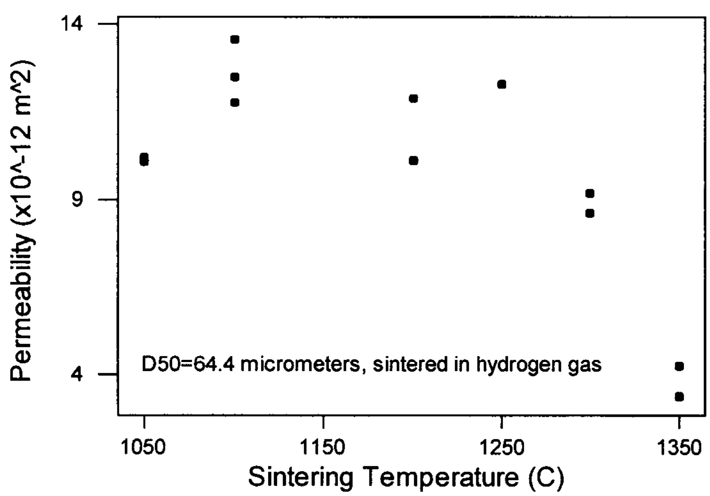


Figure 3. The effect of sintering temperature on the permeability of selective laser sintered D50=64.4 μm 316 stainless steel powder.

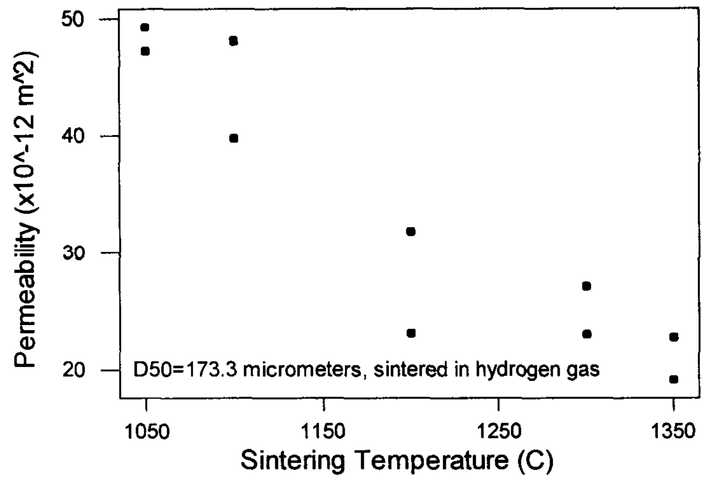


Figure 4. The effect of sintering temperature on the permeability of selective laser sintered D50=173.3 μm 316 stainless steel powder.

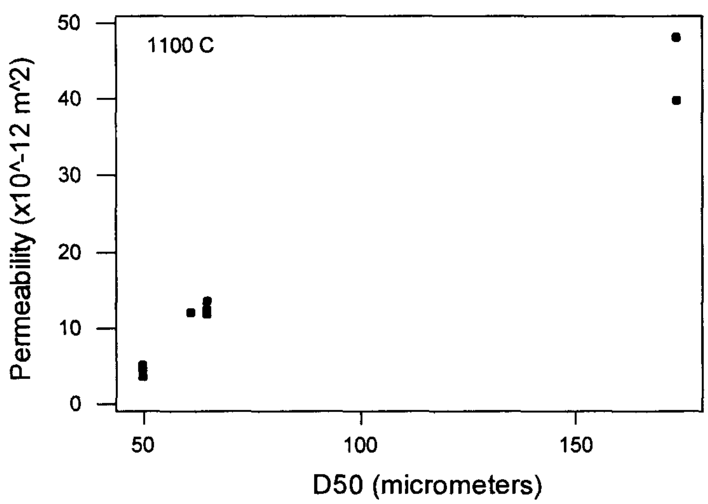


Figure 5. The effect of powder size on the permeability of SLS 316 stainless steel powders sintered at 1100°C.

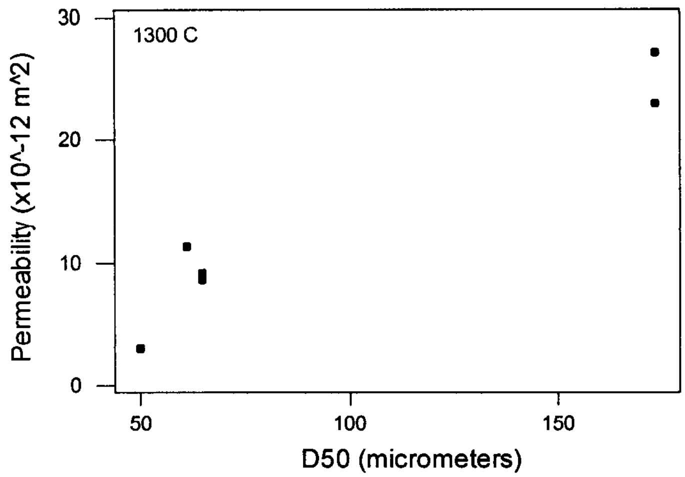


Figure 6. The effect of powder size on the permeability of SLS 316 stainless steel powders sintered at 1300°C.

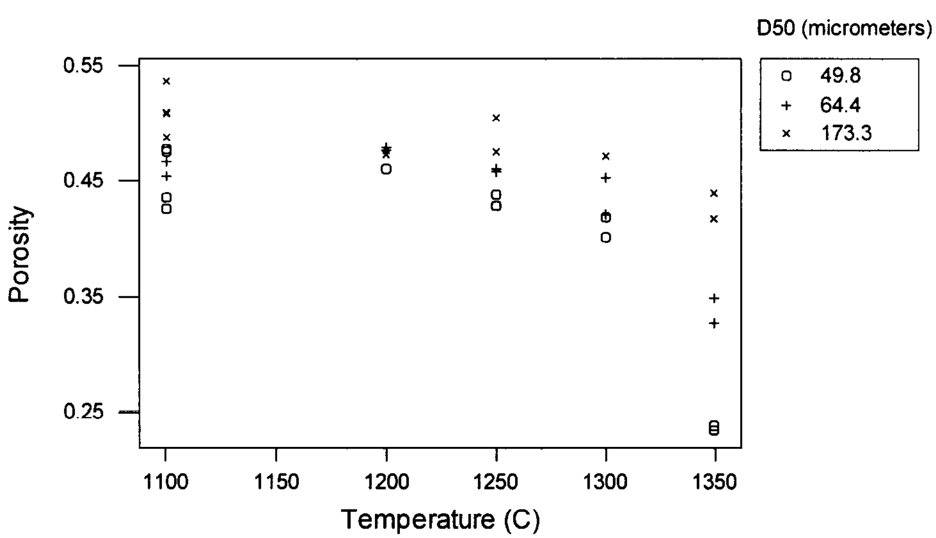


Figure 7. The effect of sintering temperature on the porosity of different sized powders.

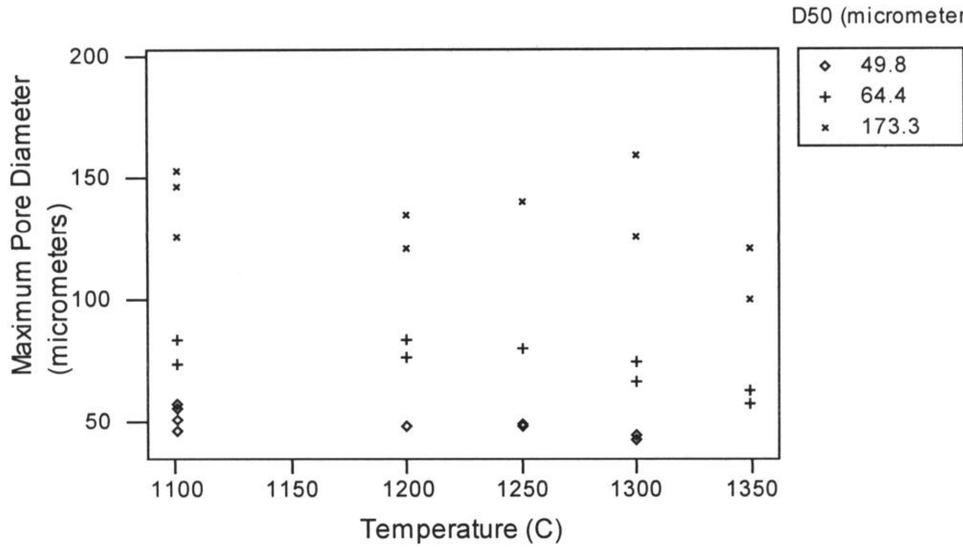


Figure 8. The effect of sintering temperature on the porosity of different sized gas atomized powders.

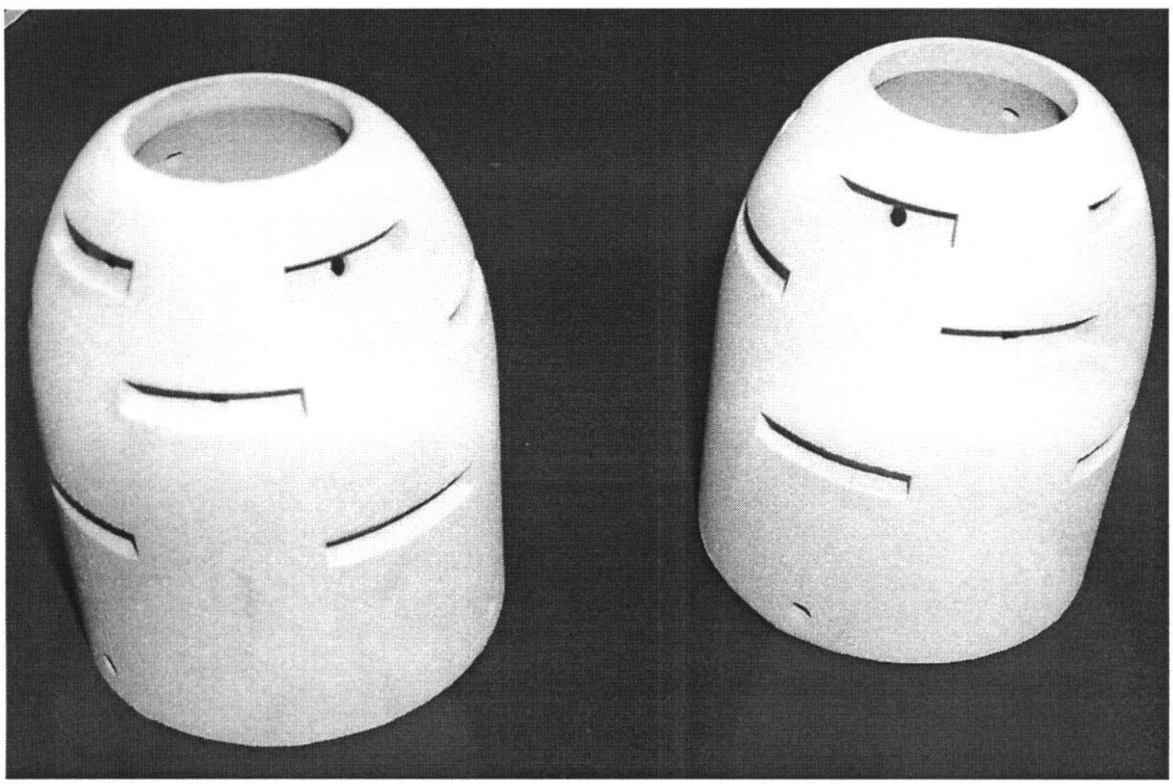

Figure 9. Net shape porous stainless steel components for fluid flow control applications.

ACKNOWLEDGEMENTS
This work was partially supported by the Center for Innovative Sintered Product at Penn State University and also from a subcontract from the Penn State University Applied Research Laboratory under contract with the Office of Naval Research, Code 333, Dr. Kam Ng, contract monitor.

REFERENCES

[1] Mark Eisenmann, "Porous Powder Metallurgy Technology", *ASM Handbook, Powder Metal Technology and Applications*, Vol. 7, 1998, pp. 1031-1042.
[2] U S Patent No. 4,944,817 and 5,076,869.
[3] R. M German, "Porous Materials", *Advances in Powder Technology*, compiled by Gilbert Y Chin, ASM Materials, 1988, pp. 225-251.